A Novel Approach for Determining Pull-In Voltages in Micro-electro-mechanical Systems (MEMS)

D.S. Long*, M.A. Shannon** and N.R. Aluru***

*University of Illinois at Urbana-Champaign
Research Assistant, Department of Mechanical Engineering
140 MEB, 1206 West Green St.,Urbana,IL,61801,dslong@uiuc.edu
**Assistant Professor, Department of Mechanical Engineering, mas1@uiuc.edu
***Assistant Professor, Department of General Engineering, aluru@uiuc.edu

ABSTRACT

In this paper we introduce a novel method, based on the Lagrange Multiplier Method (LMM), for calculating pull-in voltages in MEMS. This method combines the finite-element with a displacement constraint and boundary element method. The sign of the lagrange multiplier will be the criterion used to identify when the conductors come into contact. The validity of this numerical approach is demonstrated by two simple examples along with comparison to previously published data.

Keywords: MEMS, Lagrange Multiplier Method, Pull-In Voltage, Two-Dimensional Electrostatic Analysis.

1 INTRODUCTION

The demand for new computational techniques or even the improvement of existing ones is still needed in the MEMS community [1]. The simulation of electrostatically actuated MEMS consists of the close coupling of electrostatic and mechanical forces. A key parameter used to judge the performance of these devices is the voltage needed to cause the conductors to first come into contact (i.e. the pull-in voltage).

A common method for achieving a self-consistent solution in coupled electromechanics is the relaxation method. The method is chosen for both its simplicity and ease of integration into commercial CAD programs. Unfortunately, the determination of pull-in voltages is based on the slow or non-convergent behavior of the algorithm near pull-in [2]. Consequently, the actual pull-in voltage or the decision that pull-in has occurred due to the algorithm's slow convergence may lead to large errors in the predicted pull-in voltage. The LMM algorithm presented in this paper provides a convergent method for calculating pull-in voltages with confidence and accuracy.

This paper is organized in the following manner: electrostatic analysis is presented in Section 2, elastostatic and the LMM method is described in Section 3, the pull-in voltage algorithm is outlined in Section 5, numerical results are included in Section 6, and finally conclusions are given in Section 7.

2 ELECTROSTATIC SIMULATION

The conductor potentials in the electrostatic simulation are specified, and in the absence of free electric charges the potential must satisfy the Laplace equation

$$\nabla^2 \Psi = 0 \tag{1}$$

in the region exterior to the conductors. The charge on the surface of each conductor can be calculated by solving the integral equation for two-dimensional electrostatic analysis [3],

$$\psi(x) = -\int_s \frac{\sigma(x')}{2\pi\epsilon} \ln \|x - x'\| dS' + \mathrm{C} \qquad x \in S, \tag{2}$$

where $\psi(x)$ is the known conductor surface potential, σ is the surface charge density, ϵ is the material permittivity, and $x, x' \in R^2$. The constant C may be determined utilizing the fact that the total charge of the system is zero, such that

$$\int_s \sigma(x) dS = 0 \qquad x \in S. \tag{3}$$

A common approach for solving (2) and (3) for σ and C is to use a constant collocation scheme [2]. This scheme involves discretizing the surfaces of the conductors into a total of n panels on which the unknown surface charge density, σ, is assumed to be uniform. The result of this method will be a dense linear system of equations involving $n+1$ unknowns,

$$[\tilde{P}]\{\tilde{\sigma}\} = \{\tilde{\psi}\}, \tag{4}$$

where $\tilde{P}$ is the augmented potential coefficient matrix with $\tilde{P} \in R^{(n+1)\times(n+1)}$, and $\tilde{\sigma}$ and $\tilde{\psi}$ are the augmented surface charge density and applied potential vectors, respectively with $\tilde{\sigma}, \tilde{\psi} \in R^{n+1}$. The term augmented is used to denote the inclusion of the additional equation needed to calculate C. Upon the solution of (4), the surface charge density on each conductor will be known

and the electrostatic pressure, F_E, on the surface of each conductor is given by

$$F_E = \frac{1}{2}\frac{\sigma^2}{\epsilon}. \tag{5}$$

Once F_E has been calculated the electrostatic analysis is complete, the pressure can then be applied as a Neumann boundary condition in the LMM that will be discussed in the next section.

3 LAGRANGE MULTIPLIER METHOD FORMULATION

The motion of each conductor must be subject to the principle of impenetrability of matter, a corollary of the axiom of continuity [4]. The intent of the LMM is to impose a displacement constraint that will prohibit the conductors from penetrating one another and identify when the conductors make first contact.

The strong form of the unconstrained problem is given by the quasi-static form of Cauchy's first stress equation of motion,

$$div\mathbf{T} + \rho\mathbf{b} = \mathbf{0}, \qquad in\ \Omega \tag{6}$$

along with the Dirichlet and Neumann boundary conditions, respectively, such that

$$\mathbf{u} = \bar{\mathbf{u}} \qquad \Gamma_u, \tag{7}$$

$$\mathbf{T}\,\hat{\mathbf{n}} = \bar{\mathbf{t}}_{(\hat{\mathbf{n}})} \qquad \Gamma_q, \tag{8}$$

where $\mathbf{T}$ is the Cauchy stress tensor, ρ the mass density, and $\mathbf{b}$ the body force per unit mass. The Cauchy stress tensor $\mathbf{T}$ is related to the motion by a properly invariant constitutive law. In addition, the deformation will be assumed to remain in the linear elastic regime. A standard method for solving (6) is via a potential energy functional. For brevity, the derivation of the potential energy functionals will be omitted and will only be stated. For a linear elastic continuum with zero initial stresses, the total potential energy [5] can be expressed as

$$\Pi(\mathbf{U}) = \frac{1}{2}\mathbf{U}^T\mathbf{K}\mathbf{U} - \mathbf{U}^T\mathbf{F} \tag{9}$$

along with the condition that will invoke the stationarity of Π

$$\frac{\partial\Pi}{\partial U_i} = 0 \qquad \forall\, i. \tag{10}$$

The application of (10) yields the standard matrix equation,

$$[\mathbf{K}]\{\mathbf{U}\} = \{\mathbf{F}\}, \tag{11}$$

with $\mathbf{K}$ now identified as the stiffness matrix, $\mathbf{U}$ identified as the displacement vector, and $\mathbf{F}$ as the force vector. Imposition of the displacement constraint of $\tilde{U}$ on a single degree-of-freedom (DOF) U_i requires that (9) be rewritten as [5]

$$\Pi_L(\mathbf{U}, \Lambda) = \frac{1}{2}\mathbf{U}^T\mathbf{K}\mathbf{U} - \mathbf{U}^T\mathbf{F} + \Lambda(U_i - \tilde{U}), \tag{12}$$

where Λ is the Lagrange multiplier, which is interpreted as the point force required to impose the displacement constraint, $\tilde{U}$. Upon the minimization of Π_L, a matrix equation is produced that accounts for the displacement constraint, and is given by

$$\begin{pmatrix} \mathbf{K} & \mathbf{e}_i \\ \mathbf{e}_i^T & 0 \end{pmatrix} \begin{pmatrix} \mathbf{U} \\ \Lambda \end{pmatrix} = \begin{pmatrix} \mathbf{F} \\ \tilde{U} \end{pmatrix}, \tag{13}$$

where $\mathbf{e}_i$ is a vector that has all zeros entries except for its i^{th} entry and that entry is a one. The determination of $\mathbf{U}$ and Λ in (13) is considered the solution of the LMM problem, since the Λ calculated will ensure that the displacement $\mathbf{U}$ will be consistent with the imposed displacement constraint.

4 COUPLED ELECTROMECHANICAL SIMULATION

To obtain a self-consistent solution, the relaxation method will be used to solve (4) and (11) [6]. The details of this algorithm will not be reviewed because of its simplicity and common use in MEMS simulations.

5 PULL-IN VOLTAGE SIMULATION

The critical issue in this method is the correct selection of where to impose the displacement constraint. The location for rudimentary structures such as cantilever and fixed-fixed beams is known *ab initio*.

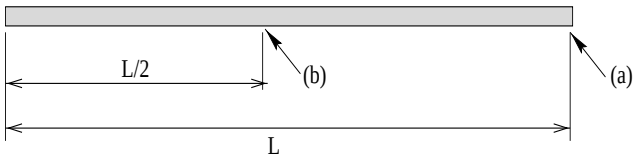

Figure 1: Location of displacement constraint on (a) cantilever beam and (b) fixed-fixed beam.

A MEMS structure in the shape of a cantilever beam over a flat rigid ground plane that is initially parallel to the beam will first come into contact at the tip or free end. As a result, the beam's displacement must be constrained at the tip, as shown in Figure 1 at point (a). Next, a fixed-fixed beam structure with a ground plane configured for the cantilever beam will first touch

the ground plane in the center. Therefore, as illustrated in Figure 1 at point (b), the beam's center displacement must be constrained. These constraints will allow the conductor's motion to be consistent with the principle of impenetrability of matter.

The constraints on the structures will be enforced exactly whether or not the applied electrostatic pressure is of sufficient magnitude to cause the conductors to come into true contact. In other words, from (12) the displacement constraint, $\tilde{U}$ (or initial gap) for DOF U_i will always be imposed. Consequently, a criterion for determining actual contact of the conductors is needed. Following the formulation in Section 3, a negative contact force is considered a false contact force and a positive contact force will be a true contact force. The sign inflection will be used to judge the when the conductors first touch or,

$$\Lambda = \begin{cases} < 0 & : \quad false\ contact \\ = 0 & : \quad first\ touch \\ > 0 & : \quad true\ contact \end{cases} . \tag{14}$$

The LMM pull-in voltage algorithm is summarized in Figure 2. The LMM algorithm leaves the standard relaxation method unchanged except for the addition of a solution step after the calculation of mechanical deformation due to the electrostatic pressure or the solution of (11). In this appended step, only linear elastic deformations are considered, leaving the stiffness matrix $\mathbf{K}$ unchanged throughout the simulation.

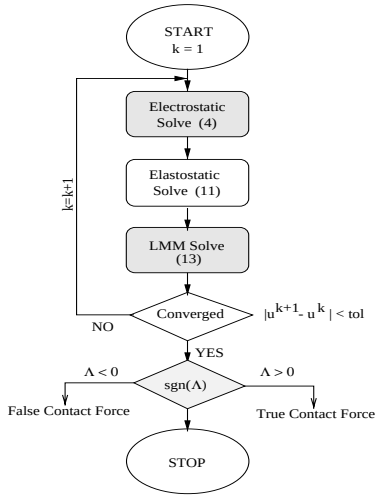

Figure 2: LMM pull-in voltage simulation flow chart with parenthetical numbers corresponding to equation numbers used in each step.

Thus, the stiffness matrix in (13) remains unchanged and will require only one initial factorization. Consequently, the simulation only requires a fast backsolve of (13) at the end of each relaxation iteration. At this point, the calculation of Λ will allow at each iteration the determination of the contact force and the voltage that produces the sign change of the contact force.

6 RESULTS

Using the methods discussed in Section 2-4, two simple electromechanical structures were analyzed. The same material properties ($E = 169GPa$ and $\nu = 0.3$) were considered for each case.

6.1 Example One:

The first example considered is a cantilever beam of the geometry shown in Figure 3. The beam is discretized into 10 8-node planar finite elements. In addition, the surface of the beam and ground plane is discretized into a total of 32 linear panels for electrostatic simulation. When a positive potential with respect to the ground plane is applied, the beam deflects towards the ground plane.

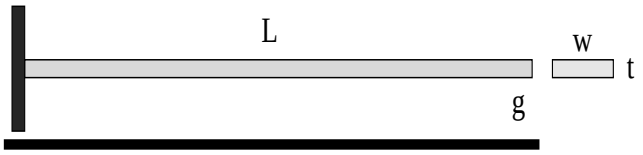

Figure 3: Cantilever beam geometry with length, $L = 80\mu m$, thickness, $t = \frac{1}{2}\mu m$, initial gap, $g = \frac{7}{10}\mu m$, and width, $w = 10\mu m$ positioned over a flat rigid ground plane.

For a bias less than the pull-in voltage, the beam reaches an equilibrium state before coming in contact with the ground plane. This equilibrium state results in a negative or false contact force as illustrated in Figure 4. As the potential difference increases, causing an increase in the electrostatic pressure, the magnitude of the contact force approaches zero. At a voltage of 2.35V a change in the contact force sign occurs as the beam's tip first touched the ground plane. This voltage is identified as the pull-in voltage, and is consistent with theoretical result of 2.33V [7], a difference of 0.86% for the same exact problem.

6.2 Example Two:

The second example considered was a fixed-fixed beam of the geometry shown in Figure 5. The beam is discretized the same as the cantilever beam example. Once again, as the potential difference is increased the distance between the beam's center and the ground plane decreased. This is verified by the decrease in the magnitude of the contact force, as illustrated in Figure 6. Also, the change in the sign of the contact force occurs when the electrostatic pressure reaches sufficient strength to

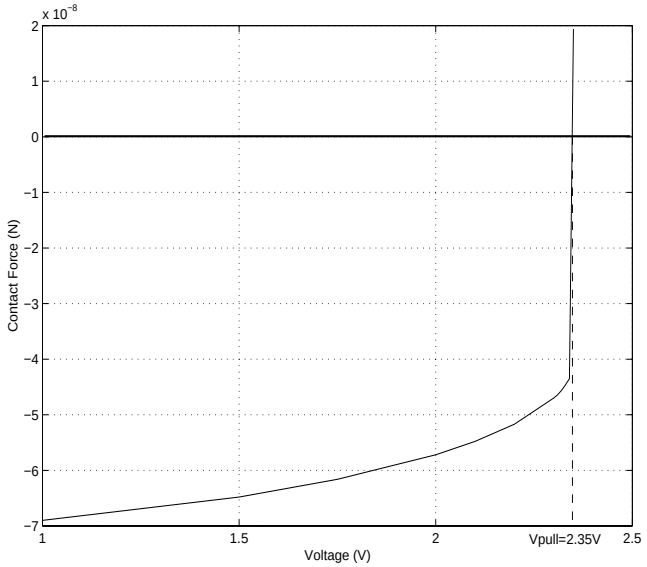

Figure 4: Pull-in voltage simulation results of cantilever beam

cause the beam to first touch the ground plane. The change in the sign of the contact force occurs at an applied potential difference of 15.39V, which is consistent with the theoretical result of 15.05V [7], a difference of 2.26% for the exact same case.

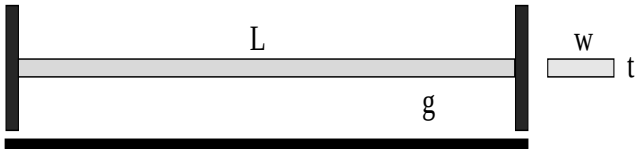

Figure 5: Fixed-fixed beam geometry with length, $L = 80\mu m$, thickness, $t = \frac{1}{2}\mu m$, initial gap, $g = \frac{7}{10}\mu m$, and width, $w = 10\mu m$ located over a flat rigid ground plane.

7 CONCLUSIONS

In this paper, the LMM was used to solve for the pull-in voltage in coupled electromechanical systems. Results from two example problems indicate that this method can be used to accurately determine the pull-in voltage. The voltages determined in the each example problem closely matched those of previously published and accepted results. The difference between the pull-in voltages calculated with this method compared to the published results can be attributed to the coarse discretization for electrostatic and elastostatic simulation. The benefit of this method over current methods of determining the pull-in voltage is that it is not based on the slow or non-convergent behavior of the relaxation method which may lead to large errors in pull-in voltages predicted. In summary, the LMM is the foundation for a promising technique for calculating pull-in voltages

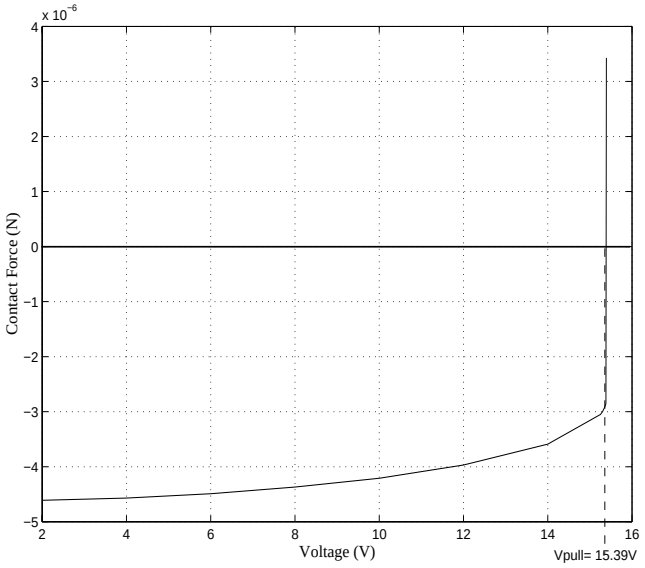

Figure 6: Pull-in voltage simulation results of fixed fixed beam.

of electromechanical devices that can be added to existing simulation tools with relative ease.

8 ACKNOWLEDGEMENT

The authors would like to thank DARPA DSO, contract DABT63-97-C-0069, for their support of this work.

REFERENCES

[1] Stephen D. Senturia, "CAD Challenges for Microsensors, Micractuators, and Microsystems," Proceedings of the IEEE, 86, 8, 1611-1626, 1998.

[2] N.R. Aluru and J. White, "An Efficient Numerical Technique for Electromechanical Simulation of Complicated Microelectromechanical Sturctures," Sensors and Actuators A, 58, 1-11, 1997.

[3] F. Shi, P. Ramesh, and S. Mukherjee, "Simulation Methods For Micro-Electro-Mechanical Structures (MEMS) With Application to a Microtweezer," Computers & Structures , 56, 5, 769-783, 1995.

[4] C. Truesdell and R. Toupin, The Classical Field Theories, In Handbuch der Physik III/1, (Edited by S. Flügge), 243-244, Springer-Verlag, 1960.

[5] Klaus-Jürgen Bathe, Finite Element Procedures, Prentice Hall, 1996.

[6] X. Cai et. al.,"A Relaxation/Multipole-Accelerated Scheme for Self-Consistent Electromechanical Analysis of Complex 3-D Microelectromechanical Sturctures", IEEE, 1993.

[7] P.M. Osterberg, S.D. Senturia, "M-TEST: A Test Chip for MEMS Material Property Measurement Using Electrostatically Actuated Test Structures", JMEMS, 6, 2, 107-118, 1997.